THE JOURNAL OF PHYSICAL CHEMISTRY Letters

Letter

Cite This: J. Phys. Chem. Lett. 2018, 9, 2305−2310

pubs.acs.org/JPCL

Vibrational Spectroscopy of Fluoroformate, FCO_2^-, Trapped in Helium Nanodroplets

Daniel A. Thomas, Eike Mucha, Sandy Gewinner, Wieland Schöllkopf, Gerard Meijer, and Gert von Helden*

Fritz-Haber-Institut der Max-Planck-Gesellschaft, Faradayweg 4-6, 14195 Berlin, Germany

Supporting Information

ABSTRACT: Fluoroformate, also known as carbonofluoridate, is an intriguing molecule readily formed by the reductive derivatization of carbon dioxide. In spite of its well-known stability, a detailed structural characterization of the isolated anion has yet to be reported. Presented in this work is the vibrational spectrum of fluoroformate obtained by infrared action spectroscopy of ions trapped in helium nanodroplets, the first application of this technique to a molecular anion. The experimental method yields narrow spectral lines, providing experimental constraints on the structure that can be accurately reproduced using high-level *ab initio* methods. In addition, two notable Fermi resonances between a fundamental and combination band are observed. The electrostatic potential map of fluoroformate reveals substantial charge density on fluorine as well as on the oxygen atoms, suggesting multiple sites for interaction with hydrogen bond donors and electrophiles, which may in turn lead to intriguing solvation structures and reaction pathways.

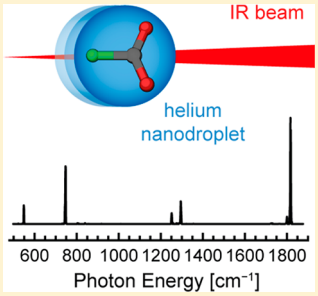

The increasing concentration of atmospheric carbon dioxide and concomitant reshaping of the earth's climate have prompted research into available routes for the reductive transformation of carbon dioxide.[1−6] Although many methods have been developed to capture carbon dioxide through sequestration or chemical conversion,[1−3] the efficient and irreversible reduction of carbon dioxide remains an elusive goal that is currently best accomplished by natural enzymes and a number of electro- and photocatalysts still under development.[5−15]

Valuable insight into the nature of CO_2-reductive activation has been gained from studying the interactions of carbon dioxide with halides and pseudohalides,[16] which have been investigated by gas-phase ion−molecule reactions,[17−21] gas-phase photodissociation spectroscopy,[22,23] photoelectron spectroscopy,[24−26] and characterization of complexes trapped as salts or within an argon matrix.[27,28] The complex between CO_2 and I^- exhibits primarily electrostatic interactions, whereas the smaller halides Br^- and Cl^- exhibit an increasing degree of charge accommodation in an antibonding orbital of the CO_2 molecule, resulting in a decreased OCO bond angle relative to that expected from interaction with a point charge.[16,23,28] This trend of increasing charge transfer with decreasing halide atomic radius continues for F^-, which forms a weak covalent bond with CO_2 to yield fluoroformate, FCO_2^-.[24] Similarly, the pseudohalide CN^- reacts with CO_2 to yield cyanoformate, $NCCO_2^-$.[29] Both of these molecules exhibit weak bonding between the halide or pseudohalide and the CO_2 moiety, with calculated lengths of ∼1.47 Å for the C−F bond in FCO_2^- and ∼1.54 Å for the C−C bond in $NCCO_2^-$.[24,28−30]

As a simple example of reductive CO_2 derivatization, fluoroformate has been investigated by numerous experimental techniques spanning several decades. McMahon and co-workers first generated gas-phase FCO_2^- by fluoride ion transfer and studied its thermochemistry by ion cyclotron resonance spectroscopy,[17,18] finding a bond dissociation enthalpy (DH_{298}) of 133 ± 8 kJ/mol, significantly weaker than typical C−F bonds (DH_{298} > 400 kJ/mol).[31] Infrared spectra of FCO_2^- trapped in an argon matrix were measured by Ault, but the presence of multiple species within the matrix hindered band assignment.[27] Zhang et al. were later able to isolate the tetramethylammonium salt of FCO_2^- and characterize its structure by infrared spectroscopy and solid-state NMR.[28] Arnold and co-workers utilized photoelectron spectroscopy to measure the electronic transitions between FCO_2^- and the fluoroformyloxyl radical, $FCO_2^{\bullet}$.[24] They also reported on the structure of FCO_2^- obtained from *ab initio* calculations, and more recent theoretical efforts yielded similar results.[29,30]

Despite the longstanding interest in the structure and properties of fluoroformate, the isolated ground-state ion has yet to be characterized experimentally. This work presents the vibrational spectrum of fluoroformate obtained by helium nanodroplet ion spectroscopy. The helium nanodroplet environment provides extremely low equilibrium temperatures approaching 0.4 K while inducing minimal spectral perturbation from helium−analyte interactions.[32] Utilizing the tunable infrared radiation produced by the free-electron laser at the Fritz Haber Institute (FHI FEL),[33] the molecule is probed across the entire anticipated range of fundamental vibrational transitions (500−1900 cm^{-1}). The infrared spectrum of

Received: March 2, 2018
Accepted: April 18, 2018
Published: April 18, 2018

Downloaded via FRITZ HABER INST DER MPI on January 28, 2021 at 10:53:41 (UTC).
See https://pubs.acs.org/sharingguidelines for options on how to legitimately share published articles.

 © 2018 American Chemical Society

DOI: 10.1021/acs.jpclett.8b00664
J. Phys. Chem. Lett. 2018, 9, 2305−2310

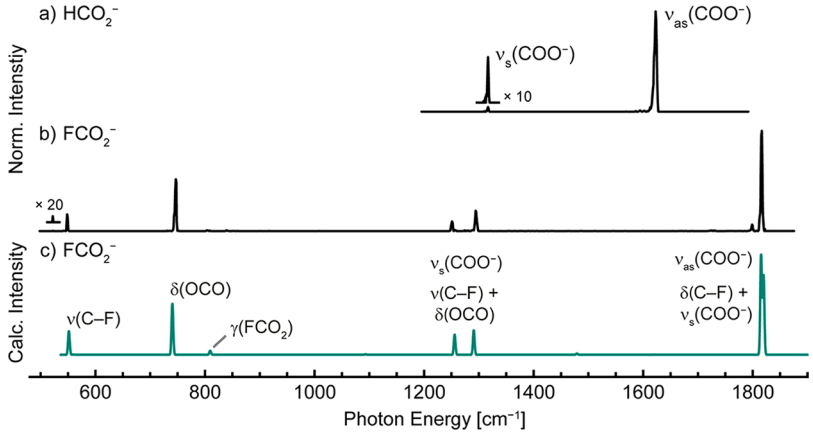

Figure 1. Vibrational spectrum of (a) formate and (b) fluoroformate obtained using the helium nanodroplet method. Shown in (c) is the theoretical vibrational spectrum of fluoroformate with anharmonic corrections (VPT2 method, CCSD(T)/aug-cc-pVTZ). Excellent agreement is observed between the experimental and theoretical vibrational spectra of fluoroformate, most notably for the Fermi resonance between $\nu_s(COO^-)$ and $\nu(C-F) + \delta(OCO)$. However, theory overestimates the degree of vibrational wave function mixing in the Fermi resonance between $\nu_{as}(COO^-)$ and $\delta(C-F) + \nu_s(COO^-)$.

formate between 1200 and 1800 cm^{-1} is also presented to provide a comparison for the normal modes of the carboxylate moiety and to corroborate the experimental methodology by comparison to literature values.

The method and instrumentation utilized to obtain vibrational spectra of ions trapped in helium nanodroplets have been described in several preceding publications.[34−36] The instrument comprises a modified commercial quadrupole time-of-flight tandem mass spectrometer with atmospheric pressure interface coupled with custom instrumentation for ion pickup by He nanodroplets and subsequent irradiation and detection. Gas-phase formate or fluoride ions were generated utilizing nanoelectrospray ionization of aqueous solutions of 0.1% (v/v) formic acid or 1 mM sodium fluoride, respectively. To generate fluoroformate, the gas-phase fluoride ions were exposed to an increased partial pressure of CO_2 during ion transfer from atmospheric pressure to high vacuum. The formate or fluoroformate ions were isolated utilizing a quadrupole mass filter and directed into an orthogonal hexapole ion trap by means of a DC ion bender. A pulsed beam of helium nanodroplets (average size of ∼20 000 He atoms) produced by an Even-Lavie valve[37] cooled to 21 K was directed through the ion trap, yielding droplets containing a single ion. The high kinetic energy of the charged nanodroplets allowed them to escape the shallow axial DC potential of the ion trap and proceed to a time-of-flight extraction region, where they were exposed to infrared radiation produced by the FHI FEL. The sequential absorption of multiple resonant photons resulted in He evaporation and the production of bare ions,[34,38] which were detected by time-of-flight mass spectrometry. The infrared spectrum was obtained as the ion signal as a function of the incident photon energy, and the intensity was scaled by the measured laser macropulse energy as a first-order power correction. Although this method of action spectroscopy utilizes a multiphoton absorption process, the ions are returned to the vibrational ground state between photon absorption events via evaporative cooling of the He nanodroplet, thereby avoiding the ion heating encountered in traditional infrared multiphoton dissociation (IRMPD) spectroscopy experiments.[39,40]

The vibrational spectra of formate and fluoroformate collected utilizing the helium nanodroplet method are shown in Figures 1a and 1b, respectively. The excellent agreement between the vibrational transitions of formate observed utilizing the helium nanodroplet technique and those reported in preceding experimental and theoretical studies (within 5 cm^{-1}, Table S3) provides validation of the experimental methodology.[41−43] In the spectrum of both formate and fluoroformate, the spectral lines are narrow, exhibiting full width at half-maximum (fwhm) values of between 2 and 6 cm^{-1}. In many cases, the measured spectral line width is narrower than the bandwidth of the laser (typical fwhm of ∼0.5% of the photon energy). This phenomenon is likely the result of the bare ion generation process, which exhibits a nonlinear dependence on the photon flux.[34,38] If a flux sufficient to produce bare ions is present only at the center of the spectral distribution, then absorption features can be measured with a width narrower than the bandwidth of the laser.

A number of the observed vibrational transitions of fluoroformate can be assigned from comparison to previous experimental efforts.[27,28] The feature at 548 cm^{-1} is assigned to the C−F stretching mode, ν(C−F), which is significantly lower in energy than typical C−F stretching vibrations (>1000 cm^{-1}),[44] demonstrating the weakness of the C−F bond (Table 1). The transition with maximum intensity at 747 cm^{-1} is

Table 1. Experimental and Theoretical Values for the Vibrational Frequencies of Fluoroformate

vibration	symm. species	experiment[a]	theory[a,b]
ν(C−F)	A_1	548	551.5
δ(C−F)	B_2	-	559.3
δ(OCO)	A_1	747	740.4
$\gamma(FCO_2)$	B_1	-	809.5
$\nu_s(COO^-)$, ν(C−F) + δ(OCO)[c]	A_1	1251	1255.8
$\nu_s(COO^-)$, ν(C−F) + δ(OCO)[c]	A_1	1294	1290.7
$\nu_{as}(COO^-)$, δ(C−F) + $\nu_s(COO^-)$[c]	B_2	1799	1819.8
$\nu_{as}(COO^-)$, δ(C−F) + $\nu_s(COO^-)$[c]	B_2	1816	1815.3

[a]Values reported in wavenumbers (cm^{-1}). [b]Calculations carried out utilizing the VPT2 method at the CCSD(T)/aug-cc-pVTZ level of theory within the CFOUR computational chemistry package.[46] [c]Spectral line arising from Fermi resonance between the listed fundamental and combination band.

DOI: 10.1021/acs.jpclett.8b00664
J. Phys. Chem. Lett. 2018, 9, 2305−2310

assigned to the OCO bending mode, δ(OCO), which agrees well with the value of 752 cm^{-1} measured previously for the fluoroformate tetramethylammonium salt and is also similar to the frequency of the OCO bending mode of formate (743 cm^{-1}) .[28,41,45] The strong feature at 1816 cm^{-1} is readily ascribed to the carboxylate asymmetric stretch of fluoroformate, $\nu_{as}(COO^-)$, slightly higher in energy than the absorption maximum at 1798 cm^{-1} measured by Zhang and co-workers for the tetramethylammonium salt.[28] Notably, this band is strongly blue-shifted from the carboxylate asymmetric stretch of formate at 1623 cm^{-1}, reflecting an increase in the OCO bond angle and decrease in the C−O bond length.

Although only a single vibrational transition is expected in the carboxylate symmetric stretch region near 1275 cm^{-1},[28] two features with maxima at 1251 and 1294 cm^{-1} are observed in the spectrum obtained by the helium nanodroplet method. Notably, the combination band of the C−F stretching mode and the OCO bending mode, ν(C−F) + δ(OCO), is predicted near 1295 cm^{-1}. This mode and $\nu_s(COO^-)$ both belong to the A_1 symmetry species of the C_{2v} point group, and the two features observed can therefore be attributed to a Fermi resonance between ν(C−F) + δ(OCO) and $\nu_s(COO^-)$.

The weak feature with maximum at 1799 cm^{-1} can similarly be expected to result from a Fermi resonance between the carboxylate asymmetric stretch, $\nu_{as}(COO^-)$, which belongs to the B_2 symmetry species, and a combination band or overtone. The combination band of δ(C−F) and $\nu_s(COO^-)$ also belongs to the B_2 symmetry species, and Fermi resonance with $\nu_{as}(COO^-)$ results in the observation of two spectral lines at 1799 and 1816 cm^{-1}.

The two Fermi doublets can be further analyzed utilizing first-order degenerate perturbation theory (see Supporting Information).[47−49] From the experimentally observed intensities and frequencies of the two Fermi doublets, one can derive the energetic spacing of the deperturbed vibrational levels as well as the interaction parameter (also referred to as the coupling constant) for each resonant pair. This analysis yields similar values for the spacing of the deperturbed vibrational levels (15 cm^{-1}) but large differences in the interaction parameter for the two doublets, with a value of 20 cm^{-1} for the resonance between $\nu_s(COO^-)$ and ν(C−F) + δ(OCO) and a value of 4 cm^{-1} for the resonance between $\nu_{as}(COO^-)$ and δ(C−F) + $\nu_s(COO^-)$. The calculated values of the deperturbed vibrational energy levels can also be utilized to estimate the frequency of the δ(C−F) fundamental, yielding a value of 520 cm^{-1}. Indeed, an extremely weak but reproducible feature is observed experimentally at 522 cm^{-1} (Figure 1), which may correspond to the fundamental of δ(C−F). This band and other low-intensity spectral lines are discussed in more detail in the Supporting Information.

Shown in Figure 1c is the theoretical anharmonic vibrational spectrum of fluoroformate, presented as the calculated vibrational transition frequencies and intensities convoluted with Gaussian distributions 3.5 cm^{-1} in width (fwhm). The frequency and intensity of fundamental transitions as well as overtones and combination bands were calculated utilizing the VPT2 method[50−53] at the CCSD(T)/aug-cc-pVTZ level of theory[54−58] as implemented within CFOUR.[46,59] This approach yields excellent agreement between experiment and theory, even for the prominent Fermi resonance between $\nu_s(COO^-)$ and ν(C−F) + δ(OCO). However, the frequency of δ(C−F) is overpredicted by this method (559 cm^{-1} vs 520 cm^{-1} from Fermi resonance analysis), resulting in an overestimation of the degree of vibrational wave function mixing in the Fermi resonance between $\nu_{as}(COO^-)$ and δ(C−F) + $\nu_s(COO^-)$. The anharmonic vibrational frequencies of fluoroformate were also determined utilizing MP2,[60,61] B3LYP,[62−65] CAM-B3LYP,[66] and PBE0[67−69] generalized VPT2 calculations[70−74] within Gaussian 09,[75] and these methods were found to yield poorer agreement with the experimental results (Figure S2, Table S2).

To study the charge distribution among the central carbon and its substituent atoms, the electrostatic potential surface of fluoroformate was calculated utilizing MOLDEN[76] as shown in Figure 2. The region around the central carbon is electron-poor

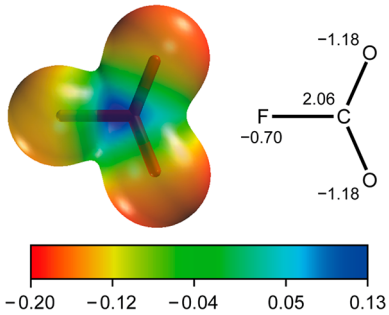

Figure 2. Electrostatic potential map of fluoroformate (atomic units, au) projected onto the total electron density isosurface (0.03 au) calculated at the CCSD(T)/aug-cc-pVTZ level of theory. Partial atomic charges (au) derived from Connolly surface fitting of the electrostatic potential surface are shown on the right. The region around the carbon atom is relatively electron-poor, whereas the three substituent atoms are relatively electron-rich.

due to the electron-withdrawing effect of both the oxygen and fluorine atoms. Structurally analogous molecules that can likewise be classified as anion-CO_2 reaction products, such as formate,[43] hydrogen carbonate,[77] and cyanoformate,[29] share this property. However, the latter molecules exhibit excess charge localization primarily on the two oxygens of the carboxylate moiety, whereas in fluoroformate substantial charge density is also found on the fluorine atom, as evidenced by the partial atomic charges derived from Connolly surface fitting to the electrostatic potential (Figure 2, Table S14).[78] In this regard, fluoroformate more closely resembles the isoelectronic molecule nitryl fluoride, FNO_2.[79] Because of this electron density distribution, electrophiles may readily interact with any of the three substituent atoms instead of preferentially with the carboxylate motif, which may influence the reactivity and solvation of fluoroformate substantially.

In summary, this work utilizes vibrational spectroscopy of ions trapped in helium nanodroplets to characterize in detail the structure and properties of isolated fluoroformate. The experimental methodology yields well-resolved vibrational transitions that are utilized in combination with theory to analyze the structure of fluoroformate. The low frequency of ν(C−F) is consistent with an anomalously long C−F bond length (theoretical value of 1.46 Å), and the large difference in frequency (>500 cm^{-1}) between the symmetric and asymmetric carboxylate stretches indicates a deformation of the OCO bond angle toward a more linear geometry (calculated value of 136.7°). In addition, this molecule exhibits two prominent Fermi resonances between a fundamental transition and combination band. Finally, the calculated electrostatic potential displays an electron-poor carbon with significant charge density

DOI: 10.1021/acs.jpclett.8b00664
J. Phys. Chem. Lett. 2018, 9, 2305−2310

on both the fluorine and oxygen atoms, suggesting electrophilic moieties may interact at any of these sites instead of preferentially at the carboxylate group. We note that this work represents the first infrared spectroscopic characterization of anion-doped helium nanodroplets. Previous experimental and theoretical efforts have reported strikingly different solvation structures for cationic vs anionic mono- and diatomic species,[80−85] but we find no qualitative experimental differences in working with molecular cations and anions. The properties of polyatomic anions in helium nanodroplets have not yet been investigated in detail, and future studies are necessary to better understand their solvation structure.

■ ASSOCIATED CONTENT

Supporting Information

The Supporting Information is available free of charge on the ACS Publications website at DOI: 10.1021/acs.jpclett.8b00664.

Discussion of low-intensity spectral features, details of Fermi resonance analysis, vibrational frequencies and intensities, structural parameters, and partial atomic charges (PDF)

■ AUTHOR INFORMATION

Corresponding Author

*E-mail: helden@fhi-berlin.mpg.de.

ORCID

Daniel A. Thomas: 0000-0001-9415-5991

Wieland Schöllkopf: 0000-0003-0564-203X

Gert von Helden: 0000-0001-7611-8740

Notes

The authors declare no competing financial interest.

■ ACKNOWLEDGMENTS

D.A.T. gratefully acknowledges the support of the Alexander von Humboldt Foundation.

■ REFERENCES

(1) Haszeldine, R. S. Carbon Capture and Storage: How Green Can Black Be? *Science* **2009**, *325*, 1647−1652.

(2) Appel, A. M.; Bercaw, J. E.; Bocarsly, A. B.; Dobbek, H.; DuBois, D. L.; Dupuis, M.; Ferry, J. G.; Fujita, E.; Hille, R.; Kenis, P. J. A.; Kerfeld, C. A.; Morris, R. H.; Peden, C. H. F.; Portis, A. R.; Ragsdale, S. W.; Rauchfuss, T. B.; Reek, J. N. H.; Seefeldt, L. C.; Thauer, R. K.; Waldrop, G. L. Frontiers, Opportunities, and Challenges in Biochemical and Chemical Catalysis of CO_2 Fixation. *Chem. Rev.* **2013**, *113*, 6621−6658.

(3) Murphy, L. J.; Robertson, K. N.; Kemp, R. A.; Tuononen, H. M.; Clyburne, J. A. C. Structurally Simple Complexes of CO_2. *Chem. Commun.* **2015**, *51*, 3942−3956.

(4) Costentin, C.; Robert, M.; Saveant, J.-M. Catalysis of the Electrochemical Reduction of Carbon Dioxide. *Chem. Soc. Rev.* **2013**, *42*, 2423−2436.

(5) Rakowski Dubois, M.; Dubois, D. L. Development of Molecular Electrocatalysts for CO_2 Reduction and H_2 Production/Oxidation. *Acc. Chem. Res.* **2009**, *42*, 1974−1982.

(6) Morris, A. J.; Meyer, G. J.; Fujita, E. Molecular Approaches to the Photocatalytic Reduction of Carbon Dioxide for Solar Fuels. *Acc. Chem. Res.* **2009**, *42*, 1983−1994.

(7) Chen, L.; Guo, Z.; Wei, X.-G.; Gallenkamp, C.; Bonin, J.; Anxolabéhère-Mallart, E.; Lau, K.-C.; Lau, T.-C.; Robert, M. Molecular Catalysis of the Electrochemical and Photochemical Reduction of CO_2 with Earth-Abundant Metal Complexes. Selective Production of CO vs HCOOH by Switching of the Metal Center. *J. Am. Chem. Soc.* **2015**, *137*, 10918−10921.

(8) Pokharel, U. R.; Fronczek, F. R.; Maverick, A. W. Reduction of Carbon Dioxide to Oxalate by a Binuclear Copper Complex. *Nat. Commun.* **2014**, *5*, 5883−5887.

(9) Sato, S.; Morikawa, T.; Kajino, T.; Ishitani, O. A Highly Efficient Mononuclear Iridium Complex Photocatalyst for CO_2 Reduction under Visible Light. *Angew. Chem., Int. Ed.* **2013**, *52*, 988−992.

(10) Chen, Y.; Li, C. W.; Kanan, M. W. Aqueous CO_2 Reduction at Very Low Overpotential on Oxide-Derived Au Nanoparticles. *J. Am. Chem. Soc.* **2012**, *134*, 19969−19972.

(11) Yu, J.; Low, J.; Xiao, W.; Zhou, P.; Jaroniec, M. Enhanced Photocatalytic CO_2-Reduction Activity of Anatase TiO_2 by Coexposed {001} and {101} Facets. *J. Am. Chem. Soc.* **2014**, *136*, 8839−8842.

(12) Li, C. W.; Kanan, M. W. CO_2 Reduction at Low Overpotential on Cu Electrodes Resulting from the Reduction of Thick Cu_2O Films. *J. Am. Chem. Soc.* **2012**, *134*, 7231−7234.

(13) Fu, Y.; Sun, D.; Chen, Y.; Huang, R.; Ding, Z.; Fu, X.; Li, Z. An Amine-Functionalized Titanium Metal−Organic Framework Photocatalyst with Visible-Light-Induced Activity for CO_2 Reduction. *Angew. Chem., Int. Ed.* **2012**, *51*, 3364−3367.

(14) Lin, S.; Diercks, C. S.; Zhang, Y.-B.; Kornienko, N.; Nichols, E. M.; Zhao, Y.; Paris, A. R.; Kim, D.; Yang, P.; Yaghi, O. M.; Chang, C. J. Covalent Organic Frameworks Comprising Cobalt Porphyrins for Catalytic CO_2 Reduction in Water. *Science* **2015**, *349*, 1208−1213.

(15) Schuchmann, K.; Müller, V. Direct and Reversible Hydrogenation of CO_2 to Formate by a Bacterial Carbon Dioxide Reductase. *Science* **2013**, *342*, 1382−1385.

(16) Weber, J. M. The Interaction of Negative Charge with Carbon Dioxide − Insight into Solvation, Speciation and Reductive Activation from Cluster Studies. *Int. Rev. Phys. Chem.* **2014**, *33*, 489−519.

(17) McMahon, T. B.; Northcott, C. J. The Fluoroformate Ion, FCO_2^-. An Ion Cyclotron Resonance Study of the Gas Phase Lewis Acidity of Carbon Dioxide and Related Isoelectronic Species. *Can. J. Chem.* **1978**, *56*, 1069−1074.

(18) Larson, J. W.; McMahon, T. B. Fluoride and Chloride Affinities of Main Group Oxides, Fluorides, Oxofluorides, and Alkyls. Quantitative Scales of Lewis Acidities from Ion Cyclotron Resonance Halide-Exchange Equilibria. *J. Am. Chem. Soc.* **1985**, *107*, 766−773.

(19) Larson, J. W.; Szulejko, J. E.; McMahon, T. B. Gas-Phase Lewis Acid-Base Interactions. An Experimental Determination of Cyanide Binding Energies from Ion Cyclotron Resonance and High-Pressure Mass Spectrometric Equilibrium Measurements. *J. Am. Chem. Soc.* **1988**, *110*, 7604−7609.

(20) Hiraoka, K.; Mizuse, S.; Yamabe, S. Stability and Structure of Cluster Ions: Halide Ions with CO_2. *J. Chem. Phys.* **1987**, *87*, 3647−3652.

(21) Hiraoka, K.; Shoda, T.; Morise, K.; Yamabe, S.; Kawai, E.; Hirao, K. Stability and Structure of Cluster Ions in the Gas Phase: Carbon Dioxide with Cl^-, H_3O^+, HCO_2^+, and HCO^+. *J. Chem. Phys.* **1986**, *84*, 2091−2096.

(22) Martin, J. P.; Case, A. S.; Gu, Q.; Darr, J. P.; McCoy, A. B.; Lineberger, W. C. Photofragmentation Dynamics of $ICN^-(CO_2)_n$ Clusters following Visible Excitation. *J. Chem. Phys.* **2013**, *139*, 064315.

(23) Weber, J. M.; Schneider, H. Infrared spectra of $X^-\cdot CO_2\cdot Ar$ Cluster Anions (X = Cl,Br,I). *J. Chem. Phys.* **2004**, *120*, 10056−10061.

(24) Arnold, D. W.; Bradforth, S. E.; Kim, E. H.; Neumark, D. M. Study of Halogen−Carbon Dioxide Clusters and the Fluoroformyloxyl Radical by Photodetachment of $X^-(CO_2)$ (X = I,Cl,Br) and FCO_2^-. *J. Chem. Phys.* **1995**, *102*, 3493−3509.

(25) Arnold, D. W.; Bradforth, S. E.; Kim, E. H.; Neumark, D. M. Study of $I^-(CO_2)_n$, $Br^-(CO_2)_n$, and $I^-(N_2O)_n$ Clusters by Anion Photoelectron Spectroscopy. *J. Chem. Phys.* **1995**, *102*, 3510−3518.

(26) Gómez, H.; Taylor, T. R.; Neumark, D. M. Anion Photoelectron Spectroscopy of $I_2^-(CO_2)_n$ (n = 1−8) Clusters. *J. Chem. Phys.* **2002**, *116*, 6111−6117.

(27) Ault, B. S. Matrix Isolation Investigation of the Fluoroformate Anion. *Inorg. Chem.* **1982**, *21*, 756−759.

(28) Zhang, X.; Gross, U.; Seppelt, K. Fluorocarbonate, $[FCO_2]^-$: Preparation and Structure. *Angew. Chem., Int. Ed. Engl.* **1995**, *34*, 1858−1860.

DOI: 10.1021/acs.jpclett.8b00664
J. Phys. Chem. Lett. 2018, 9, 2305−2310

(29) Murphy, L. J.; Robertson, K. N.; Harroun, S. G.; Brosseau, C. L.; Werner-Zwanziger, U.; Moilanen, J.; Tuononen, H. M.; Clyburne, J. A. C. A Simple Complex on the Verge of Breakdown: Isolation of the Elusive Cyanoformate Ion. *Science* **2014**, *344*, 75−78.
(30) Torrent-Sucarrat, M.; Varandas, A. J. C. Carbon Dioxide Capture and Release by Anions with Solvent-Dependent Behaviour: A Theoretical Study. *Chem. - Eur. J.* **2016**, *22*, 14056−14063.
(31) Blanksby, S. J.; Ellison, G. B. Bond Dissociation Energies of Organic Molecules. *Acc. Chem. Res.* **2003**, *36*, 255−263.
(32) Toennies, J. P.; Vilesov, A. F. Superfluid Helium Droplets: A Uniquely Cold Nanomatrix for Molecules and Molecular Complexes. *Angew. Chem., Int. Ed.* **2004**, *43*, 2622−2648.
(33) Schöllkopf, W.; Gewinner, S.; Junkes, H.; Paarmann, A.; von Helden, G.; Bluem, H.; Todd, A. M. M. The new IR and THz FEL facility at the Fritz Haber Institute in Berlin. *Proc. SPIE* **2015**, *9512*, 95121L.
(34) González Flórez, A. I.; Ahn, D.-S.; Gewinner, S.; Schöllkopf, W.; von Helden, G. IR Spectroscopy of Protonated Leu-enkephalin and its 18-crown-6 Complex Embedded in Helium Droplets. *Phys. Chem. Chem. Phys.* **2015**, *17*, 21902−21911.
(35) González Flórez, A. I.; Mucha, E.; Ahn, D.-S.; Gewinner, S.; Schöllkopf, W.; Pagel, K.; von Helden, G. Charge-Induced Unzipping of Isolated Proteins to a Defined Secondary Structure. *Angew. Chem., Int. Ed.* **2016**, *55*, 3295−3299.
(36) Mucha, E.; González Flórez, A. I.; Marianski, M.; Thomas, D. A.; Hoffmann, W.; Struwe, W. B.; Hahm, H. S.; Gewinner, S.; Schöllkopf, W.; Seeberger, P. H.; von Helden, G.; Pagel, K. Glycan Fingerprinting via Cold-Ion Infrared Spectroscopy. *Angew. Chem., Int. Ed.* **2017**, *56*, 11248−11251.
(37) Even, U. The Even-Lavie Valve as a Source for High Intensity Supersonic Beam. *EPJ. Technol. Instrum.* **2015**, *2*, 17.
(38) Filsinger, F.; Ahn, D.-S.; Meijer, G.; von Helden, G. Photoexcitation of Mass/Charge Selected Hemin$^+$, Caught in Helium Nanodroplets. *Phys. Chem. Chem. Phys.* **2012**, *14*, 13370−13377.
(39) Oomens, J.; Sartakov, B. G.; Meijer, G.; von Helden, G. Gas-Phase Infrared Multiple Photon Dissociation Spectroscopy of Mass-Selected Molecular Ions. *Int. J. Mass Spectrom.* **2006**, *254*, 1−19.
(40) Polfer, N. C. Infrared Multiple Photon Dissociation Spectroscopy of Trapped Ions. *Chem. Soc. Rev.* **2011**, *40*, 2211−2221.
(41) Forney, D.; Jacox, M. E.; Thompson, W. E. Infrared Spectra of trans-HOCO, HCOOH$^+$, and HCO_2^- Trapped in Solid Neon. *J. Chem. Phys.* **2003**, *119*, 10814−10823.
(42) Krekeler, C.; Mladenovic, M.; Botschwina, P. A Theoretical Investigation of the Vibrational States of HCO_2^- and its Isotopomers. *Phys. Chem. Chem. Phys.* **2005**, *7*, 882−887.
(43) Gerardi, H. K.; DeBlase, A. F.; Su, X.; Jordan, K. D.; McCoy, A. B.; Johnson, M. A. Unraveling the Anomalous Solvatochromic Response of the Formate Ion Vibrational Spectrum: An Infrared, Ar-Tagging Study of the HCO_2^-, DCO_2^-, and $HCO_2^-{\cdot}H_2O$ Ions. *J. Phys. Chem. Lett.* **2011**, *2*, 2437−2441.
(44) Shimanouchi, T. Tables of Molecular Vibrational Frequencies. Consolidated Volume II. *J. Phys. Chem. Ref. Data* **1977**, *6*, 993−1102.
(45) Garand, E.; Klein, K.; Stanton, J. F.; Zhou, J.; Yacovitch, T. I.; Neumark, D. M. Vibronic Structure of the Formyloxyl Radical (HCO_2) via Slow Photoelectron Velocity-Map Imaging Spectroscopy and Model Hamiltonian Calculations. *J. Phys. Chem. A* **2010**, *114*, 1374−1383.
(46) CFOUR. Coupled-Cluster techniques for Computational Chemistry, a quantum-chemical program package by J.F. Stanton, J. Gauss, L. Cheng, M.E. Harding, D.A. Matthews, P.G. Szalay, with contributions from A.A. Auer, R.J. Bartlett, U. Benedikt, C. Berger, D.E. Bernholdt, Y.J. Bomble, O. Christiansen, F. Engel, R. Faber, M. Heckert, O. Heun, M. Hilgenberg, C. Huber, T.-C. Jagau, D. Jonsson, J. Jusélius, T. Kirsch, K. Klein, W.J. Lauderdale, F. Lipparini, T. Metzroth, L.A. Mück, D.P. O'Neill, D.R. Price, E. Prochnow, C. Puzzarini, K. Ruud, F. Schiffmann, W. Schwalbach, C. Simmons, S. Stopkowicz, A. Tajti, J. Vázquez, F. Wang, J.D. Watts and the integral packages MOLECULE (J. Almlöf and P.R. Taylor), PROPS (P.R. Taylor), ABACUS (T. Helgaker, H.J. Aa. Jensen, P. Jørgensen, and J. Olsen), and ECP routines by A. V. Mitin and C. van Wüllen. For the current version, see http://www.cfour.de.
(47) Herzberg, G. *Molecular Spectra and Molecular Structure II. Infrared and Raman Spectra of Polyatomic Molecules*; D. Van Nostrand: New York, 1945.
(48) Fermi, E. Über den Ramaneffekt des Kohlendioxyds. *Eur. Phys. J. A* **1931**, *71*, 250−259.
(49) Monecke, J. Theory of Fermi Resonances in Raman and Infrared Spectra. *J. Raman Spectrosc.* **1987**, *18*, 477−479.
(50) Schneider, W.; Thiel, W. Anharmonic Force Fields from Analytic Second Derivatives: Method and Application to Methyl Bromide. *Chem. Phys. Lett.* **1989**, *157*, 367−373.
(51) Stanton, J. F.; Lopreore, C. L.; Gauss, J. The Equilibrium Structure and Fundamental Vibrational Frequencies of Dioxirane. *J. Chem. Phys.* **1998**, *108*, 7190−7196.
(52) Stanton, J. F.; Gauss, J. Analytic Second Derivatives in High-Order Many-body Perturbation and Coupled-Cluster Theories: Computational Considerations and Applications. *Int. Rev. Phys. Chem.* **2000**, *19*, 61−95.
(53) Vázquez, J.; Stanton, J. F. Simple(r) Algebraic Equation for Transition Moments of Fundamental Transitions in Vibrational Second-Order Perturbation Theory. *Mol. Phys.* **2006**, *104*, 377−388.
(54) Raghavachari, K.; Trucks, G. W.; Pople, J. A.; Head-Gordon, M. A Fifth-Order Perturbation Comparison of Electron Correlation Theories. *Chem. Phys. Lett.* **1989**, *157*, 479−483.
(55) Bartlett, R. J.; Watts, J. D.; Kucharski, S. A.; Noga, J. Non-Iterative Fifth-Order Triple and Quadruple Excitation Energy Corrections in Correlated Methods. *Chem. Phys. Lett.* **1990**, *165*, 513−522.
(56) Stanton, J. F. Why CCSD(T) Works: a Different Perspective. *Chem. Phys. Lett.* **1997**, *281*, 130−134.
(57) Kendall, R. A.; Dunning, T. H., Jr.; Harrison, R. J. Electron Affinities of the First-Row Atoms Revisited. Systematic Basis Sets and Wave Functions. *J. Chem. Phys.* **1992**, *96*, 6796−6806.
(58) Woon, D. E.; Dunning, T. H., Jr. Gaussian Basis Sets for Use in Correlated Molecular Calculations. IV. Calculation of Static Electrical Response Properties. *J. Chem. Phys.* **1994**, *100*, 2975−2988.
(59) Harding, M. E.; Metzroth, T.; Gauss, J.; Auer, A. A. Parallel Calculation of CCSD and CCSD(T) Analytic First and Second Derivatives. *J. Chem. Theory Comput.* **2008**, *4*, 64−74.
(60) Møller, C.; Plesset, M. S. Note on an Approximation Treatment for Many-Electron Systems. *Phys. Rev.* **1934**, *46*, 618−622.
(61) Bartlett, R. J. Many-Body Perturbation Theory and Coupled Cluster Theory for Electron Correlation in Molecules. *Annu. Rev. Phys. Chem.* **1981**, *32*, 359−401.
(62) Lee, C.; Yang, W.; Parr, R. G. Development of the Colle-Salvetti Correlation-Energy Formula into a Functional of the Electron Density. *Phys. Rev. B: Condens. Matter Mater. Phys.* **1988**, *37*, 785−789.
(63) Becke, A. D. Density-Functional Thermochemistry. III. The Role of Exact Exchange. *J. Chem. Phys.* **1993**, *98*, 5648−5652.
(64) Stephens, P. J.; Devlin, F. J.; Chabalowski, C. F.; Frisch, M. J. Ab Initio Calculation of Vibrational Absorption and Circular Dichroism Spectra Using Density Functional Force Fields. *J. Phys. Chem.* **1994**, *98*, 11623−11627.
(65) Kim, K.; Jordan, K. D. Comparison of Density Functional and MP2 Calculations on the Water Monomer and Dimer. *J. Phys. Chem.* **1994**, *98*, 10089−10094.
(66) Yanai, T.; Tew, D. P.; Handy, N. C. A New Hybrid Exchange−Correlation Functional using the Coulomb-Attenuating Method (CAM-B3LYP). *Chem. Phys. Lett.* **2004**, *393*, 51−57.
(67) Perdew, J. P.; Burke, K.; Ernzerhof, M. Generalized Gradient Approximation Made Simple. *Phys. Rev. Lett.* **1996**, *77*, 3865−3868.
(68) Perdew, J. P.; Ernzerhof, M.; Burke, K. Rationale for Mixing Exact Exchange with Density Functional Approximations. *J. Chem. Phys.* **1996**, *105*, 9982−9985.
(69) Adamo, C.; Barone, V. Toward Reliable Density Functional Methods without Adjustable Parameters: The PBE0Model. *J. Chem. Phys.* **1999**, *110*, 6158−6170.

DOI: 10.1021/acs.jpclett.8b00664
J. Phys. Chem. Lett. 2018, 9, 2305−2310

(70) Barone, V. Anharmonic Vibrational Properties by a Fully Automated Second-Order Perturbative Approach. *J. Chem. Phys.* **2005**, *122*, 014108.
(71) Barone, V.; Bloino, J.; Guido, C. A.; Lipparini, F. A Fully Automated Implementation of VPT2 Infrared Intensities. *Chem. Phys. Lett.* **2010**, *496*, 157−161.
(72) Bloino, J.; Barone, V. A Second-Order Perturbation Theory Route to Vibrational Averages and Transition Properties of Molecules: General Formulation and Application to Infrared and Vibrational Circular Dichroism Spectroscopies. *J. Chem. Phys.* **2012**, *136*, 124108.
(73) Barone, V.; Biczysko, M.; Bloino, J. Fully Anharmonic IR and Raman Spectra of Medium-Size Molecular Systems: Accuracy and Interpretation. *Phys. Chem. Chem. Phys.* **2014**, *16*, 1759−1787.
(74) Piccardo, M.; Bloino, J.; Barone, V. Generalized Vibrational Perturbation Theory for Rotovibrational Energies of Linear, Symmetric and Asymmetric Tops: Theory, Approximations, and Automated Approaches to deal with Medium-to-Large Molecular Systems. *Int. J. Quantum Chem.* **2015**, *115*, 948−982.
(75) Frisch, M. J.; Trucks, G. W.; Schlegel, H. B.; Scuseria, G. E.; Robb, M. A.; Cheeseman, J. R.; Scalmani, G.; Barone, V.; Petersson, G. A.; Nakatsuji, H.; Li, X.; Caricato, M.; Marenich, A.; Bloino, J.; Janesko, B. G.; Gomperts, R.; Mennucci, B.; Hratchian, H. P.; Ortiz, J. V.; Izmaylov, A. F.; Sonnenberg, J. L.; Williams-Young, D.; Ding, F.; Lipparini, F.; Egidi, F.; Goings, J.; Peng, B.; Petrone, A.; Henderson, T.; Ranasinghe, D.; Zakrzewski, V. G.; Gao, J.; Rega, N.; Zheng, G.; Liang, W.; Hada, M.; Ehara, M.; Toyota, K.; Fukuda, R.; Hasegawa, J.; Ishida, M.; Nakajima, T.; Honda, Y.; Kitao, O.; Nakai, H.; Vreven, T.; Throssell, K.; Montgomery, J. A., Jr.; Peralta, J. E.; Ogliaro, F.; Bearpark, M.; Heyd, J. J.; Brothers, E.; Kudin, K. N.; Staroverov, V. N.; Keith, T.; Kobayashi, R.; Normand, J.; Raghavachari, K.; Rendell, A.; Burant, J. C.; Iyengar, S. S.; Tomasi, J.; Cossi, M.; Millam, J. M.; Klene, M.; Adamo, C.; Cammi, R.; Ochterski, J. W.; Martin, R. L.; Morokuma, K.; Farkas, O.; Foresman, J. B.; Fox, D. J. *Gaussian 09*, Revision D.01; Gaussian, Inc.: Wallingford, CT, 2009.
(76) Schaftenaar, G.; Noordik, J. H. Molden: a Pre- and Post-processing Program for Molecular and Electronic Structures. *J. Comput.-Aided Mol. Des.* **2000**, *14*, 123−134.
(77) Shusterman, A. J.; Shusterman, G. P. Teaching Chemistry with Electron Density Models. *J. Chem. Educ.* **1997**, *74*, 771.
(78) Besler, B. H.; Merz, K. M.; Kollman, P. A. Atomic Charges Derived from Semiempirical Methods. *J. Comput. Chem.* **1990**, *11*, 431−439.
(79) Legon, A. C. Tetrel, Pnictogen and Chalcogen Bonds Identified in the Gas Phase before they had Names: a Systematic Look at Non-covalent Interactions. *Phys. Chem. Chem. Phys.* **2017**, *19*, 14884−14896.
(80) Rosenblit, M.; Jortner, J. Electron Bubbles in Helium Clusters. I. Structure and Energetics. *J. Chem. Phys.* **2006**, *124*, 194505.
(81) Coccia, E.; Marinetti, F.; Bodo, E.; Gianturco, F. A. Chemical Solutions in a Quantum Solvent: Anionic Electrolytes in ^{4}He Nanodroplets. *ChemPhysChem* **2008**, *9*, 1323−1330.
(82) Coccia, E.; Marinetti, F.; Bodo, E.; Gianturco, F. A. Anionic Microsolvation in Helium Droplets: $OH^-(He)_N$ Structures from Classical and Quantum Calculations. *J. Chem. Phys.* **2008**, *128*, 134511.
(83) Ferreira da Silva, F.; Waldburger, P.; Jaksch, S.; Mauracher, A.; Denifl, S.; Echt, O.; Märk, T. D.; Scheier, P. On the Size of Ions Solvated in Helium Clusters. *Chem. - Eur. J.* **2009**, *15*, 7101−7108.
(84) Fiedler, S. L.; Mateo, D.; Aleksanyan, T.; Eloranta, J. Theoretical Modeling of Ion Mobility in Superfluid ^{4}He. *Phys. Rev. B: Condens. Matter Mater. Phys.* **2012**, *86*, 144522.
(85) Mauracher, A.; Daxner, M.; Postler, J.; Huber, S. E.; Denifl, S.; Scheier, P.; Toennies, J. P. Detection of Negative Charge Carriers in Superfluid Helium Droplets: The Metastable Anions He^{*-} and He_2^{*-}. *J. Phys. Chem. Lett.* **2014**, *5*, 2444−2449.

DOI: 10.1021/acs.jpclett.8b00664
J. Phys. Chem. Lett. 2018, 9, 2305−2310